

Differential conductance of a saddle-point constriction with a time-modulated gate-voltage

C. S. Tang¹ and C. S. Chu²

¹Physics Division, National Center for Theoretical Sciences, P.O. Box 2-131, Hsinchu 30013, Taiwan

²Department of Electrophysics, National Chiao Tung University, Hsinchu 30010, Taiwan

The effect of a time-modulated gate-voltage on the differential conductance G of a saddle-point constriction is studied. The constriction is modeled by a symmetric saddle-point potential and the time-modulated gate-voltage is represented by a potential of the form $V_0 (a=2 \sqrt{x-x_c}) \cos(\omega t)$. For $\hbar\omega$ less than half of the transverse subband energy level spacing, gate-voltage-assisted (suppressed) feature occurs when the chemical potential is less (greater) than but close to the threshold energy of a subband. As ω increases, G is found to exhibit, alternatively, the assisted and the suppressed feature. For larger $\hbar\omega$, these two features may overlap with one another. Dip structures are found in the suppressed regime. Mini-steps are found in the assisted regime only when the gate-voltage covers region far enough away from the center of the constriction.

PACS numbers: 72.10.-d, 72.40.+w

I. INTRODUCTION

The effects of time-modulated fields on the quantum transport have been of continued interest in the recent past. These time-modulated fields can be transversely polarized [1, 2, 3, 4, 5, 6, 7, 8, 9, 10], longitudinally polarized [11, 12], or represented by time-modulated potentials, with no polarization [13, 14, 15, 16, 17, 18, 19, 20, 21]. The systems recently considered are mostly mesoscopic systems, such as the narrow constrictions [1, 2, 3, 4, 5, 6, 7, 8, 9, 10, 17, 21]. For the case when a constriction is acted upon by an incident electromagnetic wave, the time-modulated field has a polarization. This situation can be realized experimentally, as is demonstrated by two latest experiments [4, 6]. On the other hand, the time-modulated potentials are expected to be realized in gate-voltage configurations [21, 22], which is shown in Fig. 1.

The presence of the time-modulated fields, with or without polarizations, gives rise to coherent inelastic scatterings. These inelastic scatterings do not conserve the longitudinal momentum along the transport direction, as long as the time-modulated fields have finite longitudinal ranges. The reason being that the finiteness in the range of the fields breaks the translational invariance [9, 21]. Furthermore, the inelastic scattering processes in-

duced by these time-modulated fields depend also on the polarization of the fields. In an adiabatically varying constriction, the inelastic scattering processes involve inter-subband transitions, when the time-modulated fields are transversely polarized, but involve only intra-subband transitions, when the fields do not have polarizations, such as those arise from time-modulated gate-voltages. The detail transport characteristics of the constriction hence depend on the polarization of the time-modulated fields.

In this work we focus on the case of a time-modulated potential. The effect of such a potential on the transport properties of one dimensional systems have been investigated in many previous works [13, 14, 15, 16, 17, 18, 19, 20, 21]. However, the possible manifestation of quasi-bound-state (QBS) features has not been widely recognized, except for the work of Bagwell and Lake [17], who have considered a time-dependent potential that has a delta profile. The energy of this QBS is below, but close to, the band bottom of the one dimensional system. The transport exhibits QBS feature when the conducting electrons can make transitions via inelastic processes to the QBS. We expect this QBS feature to be more significant in a narrow constriction than in a one dimensional system, because there are, in a constriction, more subbands and hence more QBS's. Furthermore, the tunability of the subband structures and the chemical potential together provide greater feasibility for probing the QBS feature in narrow constrictions.

In an earlier work [21], the present authors have investigated the effect of a time-dependent gate potential acting upon the uniform-width region of a narrow constriction. For those electrons that manage to enter the narrow channel region from the two end-electrodes, they have perfect transmission, and the time-modulated potential cannot further increase the dc conductance. Instead, the potential causes backscattering, and leads to lower dc conductances. Hence it is not unexpected that the dc conductance is found to exhibit only gate-voltage-

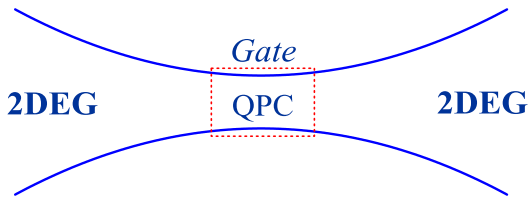


FIG. 1: Sketch of the gated saddle-point constriction which is connected at each end to a two-dimensional electron gas electrode. The gate induces a finite-range time-modulated potential in the constriction.

suppressed and not gate-voltage-assisted feature [21]. As the chemical potential increases, the suppressed feature in the dc conductance is characterized by dip structures at which ϵ is $\hbar/2$ above the threshold energy of a subband. These dip structures are associated with the formation of QBS at a subband bottom in the narrow channel due partly to the singular density of states (DOS). It is interesting to see whether such QBS feature persists in systems that have large but not singular DOS, and to explore cases that may have gate-voltage-assisted feature.

These questions motivate us to study a saddle-point constriction in the presence of a time-modulated gate-voltage. A few interesting issues are addressed. First of all, the effective DOS in a saddle-point constriction is not singular. This is because the singularity in the DOS of a narrow channel comes from both the one-dimensionality and the sharp threshold energy of each subband. In a saddle-point constriction, the threshold energy of each subband is not sharp but is smeared by tunneling processes that occur near the threshold. The robustness of the QBS feature against the absence of a singular DOS is explored. Second, the gate-voltage covers regions in which the effective width of the constriction is varying. The gate-voltage-assisted processes become possible, which should be sensitive to the range of the gate-voltage. These range-dependent characteristics are studied. Third, the system can easily be configured into an asymmetric situation by shifting the center of the gate-voltage away from the symmetric center of the saddle-point constriction. The effect of this asymmetry is studied.

In Sec. II we present our method. In Sec. III we present some numerical examples. A conclusion is presented in Sec. IV.

II. THEORY

Choosing the energy unit $E = \hbar^2 k_F^2 / 2m$, the length unit $a = 1/k_F$, the time unit $t = \hbar/E$, and V_0 in units of E , the dimensionless Schrodinger equation for such saddle-point constriction becomes

$$i \frac{\partial}{\partial t} (\mathbf{x}; t) = -\nabla^2 + \nabla_x^2 x^2 + \nabla_y^2 y^2 + V(\mathbf{x}; t) \quad (\mathbf{x}; t); \quad (1)$$

Here k_F is a typical Fermi wave vector of the reservoir and m is the effective mass. The transverse energy levels $\epsilon_n = (2n+1)/2$ are quantized, with $\phi_n(y)$ being the corresponding wave functions. The time-modulated gate-voltage $V(\mathbf{x}; t)$ is given by

$$V(\mathbf{x}; t) = V_0 \frac{a}{2} |x - x_c| \cos(\omega t); \quad (2)$$

where the interaction region is centered at x_c and with a longitudinal range a . Even though the saddle-point constriction is symmetric, the transport characteristics could become asymmetric if the interaction region were not centered at the symmetric center of the constriction. On the other hand, the $V(\mathbf{x}; t)$ we considered is uniform

in the transverse direction and it does not induce inter-subband transitions. Thus for a n th subband electron, and with energy ϵ , incident along \hat{x} , the subband index n remains unchanged and the scattering wave function can be written in the form $\psi_n^+(\mathbf{x}; t) = \phi_n(y) \psi_n^+(x; t)$.

The wave function $\psi_n^+(\mathbf{x}; t)$ can be expressed in terms of the unperturbed wave functions $\phi_n(y)$ which satisfy the Schrodinger equation

$$-\frac{\partial^2}{\partial y^2} \phi_n^2(x^2) \phi_n^2(y) = \epsilon_n \phi_n^2(y); \quad (3)$$

where $\epsilon_n = \frac{1}{2}(2n+1)$ is the energy for the motion along \hat{x} . The solutions to Eq. (3) are doubly degenerate, given by [23]

$$\begin{aligned} \psi_e(\mathbf{x}; n) &= \exp \left(-\frac{i \epsilon_n x^2}{2} \right) \\ &M \left(\frac{1}{4} + i \frac{n}{4 \epsilon_n}; \frac{1}{2}; i \epsilon_n x^2 \right); \end{aligned} \quad (4)$$

and

$$\begin{aligned} \psi_o(\mathbf{x}; n) &= x^p \exp \left(-\frac{i \epsilon_n x^2}{2} \right) \\ &M \left(\frac{3}{4} + i \frac{n}{4 \epsilon_n}; \frac{3}{2}; i \epsilon_n x^2 \right); \end{aligned} \quad (5)$$

Here, $\psi_e(\mathbf{x})$ is an even (odd) function of x , and $M(a; b; z)$ is the Kummer function [24]. For our scattering problem, it is more convenient to construct out of ψ_e and ψ_o wave functions that have the appropriate asymptotic behaviors. In the asymptotic region $x \rightarrow -1$, we construct wave functions ψ_{in} and ψ_{ref} which have only positive and negative current, respectively. In the asymptotic region $x \rightarrow +1$, we construct wave function ψ_{tran} which has only positive current. These wave functions are given by [23]

$$\psi_{in}(\mathbf{x}; n) = \psi_o(\mathbf{x}; n) + (-1)^n \psi_e(\mathbf{x}; n); \quad (6)$$

$$\psi_{ref}(\mathbf{x}; n) = \psi_o(\mathbf{x}; n) + (-1)^n \psi_e(\mathbf{x}; n); \quad (7)$$

and

$$\psi_{tran}(\mathbf{x}; n) = \psi_o(\mathbf{x}; n) + (-1)^n \psi_e(\mathbf{x}; n); \quad (8)$$

where

$$\begin{aligned} (-1)^n &= \frac{1}{4} \exp \left(-\frac{n}{4 \epsilon_n} \right) i \exp \left(\frac{n}{4 \epsilon_n} \right) \\ &\frac{1}{4} + i \frac{n}{4 \epsilon_n}; \end{aligned} \quad (9)$$

and $\Gamma(z)$ is the Gamma function.

Using these wave functions, the wave function $\psi(\mathbf{x}; t)$ that corresponds to an electron incident from the left hand side of the constriction can be written in the form [14, 21]

$$\begin{aligned}
\psi(x;t) &= \psi_{in}(x; n) e^{i t} + \sum_m r_m^{(+)}(n; x_c) \psi_{ref}(x; n+m!) e^{i(n+m!)t}; \text{ if } x < x_0 \\
\psi(x;t) &= \sum_m \left[A(m) \psi_{ref}(x; n) + B(m) \psi_{tran}(x; n) \right] e^{i t} \\
&\quad + \sum_p J_p \frac{V_0}{!} e^{i p t}; \text{ if } x_0 < x < x_1 \\
\psi(x;t) &= \sum_m t_m^{(+)}(n; x_c) \psi_{tran}(x; n+m!) e^{i(n+m!)t}; \text{ if } x > x_1
\end{aligned} \tag{10}$$

where n is the subband index, m is the sideband index, and $J_p(x)$ is the Bessel function. The superscript $(+)$ in the transmission and the reflection coefficients indicates that the electron is incident from the left hand side of the constriction. The sideband index m corresponds to a net energy change of $m\hbar\omega$ for the outgoing electrons. The two ends of the interaction region are at $x_0 = x_c - a/2$ and $x_1 = x_c + a/2$.

The transmission and the reflection coefficients can be obtained from matching the wave functions and their derivatives at the two ends of the time-modulated gate-voltage. For the matching to hold at all times, the integration variable in Eq. (10) has to take on discrete

values $m!$. Hence we can write $A(m)$ and $B(m)$ in the form

$$F(m) = \sum_m F(m!) (n+m!); \tag{11}$$

where $F(m)$ refers to either $A(m)$ or $B(m)$. After performing the matching and eliminating the reflection coefficients $r_m^{(+)}(n; x_c)$, we obtain the equations relating $A(m)$, $B(m)$ and the transmission coefficients $t_m^{(+)}(n; x_c)$, given by

$$\begin{aligned}
\psi_{tran}(x_1; n+m!) t_m^{(+)}(n; x_c) &= \sum_{m^0} [A(m^0) \psi_{ref}(x_1; n+m^0!) + B(m^0) \psi_{tran}(x_1; n+m^0!)] \\
&\quad J_{m-m^0} \frac{V_0}{!}; \tag{12}
\end{aligned}$$

$$\begin{aligned}
\psi_{tran}^0(x_1; n+m!) t_m^{(+)}(n; x_c) &= \sum_{m^0} [A(m^0) \psi_{ref}^0(x_1; n+m^0!) + B(m^0) \psi_{tran}^0(x_1; n+m^0!)] \\
&\quad J_{m-m^0} \frac{V_0}{!}; \tag{13}
\end{aligned}$$

and

$$\begin{aligned}
&[\psi_{in}(x_0; n) \psi_{ref}^0(x_0; n) - \psi_{in}^0(x_0; n) \psi_{ref}(x_0; n)]_{m=0} \\
&= \sum_{m^0} [\psi_{ref}(x_0; n+m^0!) \psi_{ref}^0(x_0; n+m!) - \psi_{ref}^0(x_0; n+m^0!) \psi_{ref}(x_0; n+m!)] \\
&\quad + A(m^0) J_{m-m^0} \frac{V_0}{!} \\
&+ \sum_{m^0} [\psi_{tran}(x_0; n+m^0!) \psi_{ref}^0(x_0; n+m!) - \psi_{tran}^0(x_0; n+m^0!) \psi_{ref}(x_0; n+m!)] \\
&\quad + B(m^0) J_{m-m^0} \frac{V_0}{!}; \tag{14}
\end{aligned}$$

where $\psi^0 = \psi|_{x=x_c}$.

Solving Eqs. (12)-(14), we obtain $t_m^{(+)}(n; x_c)$; $A(m)$;

and $B(m)$, from which the reflection coefficients $r_m^{(+)}(n; x_c)$ can be calculated. The corresponding coefficients for electrons incident from the right hand side of the constriction can be found following similar procedure. The correctness of the transmission and the reflection coefficients can be checked by a conservation of current condition, given by

$$\sum_m \frac{\frac{1}{4} + i \frac{n+m}{4!x}}{\frac{1}{4} + i \frac{n}{4!x}} \exp \frac{m}{4!x} \frac{m!}{4!x} \frac{i}{j_m^{(+)}(n; x_c) f_j + j_m^{(-)}(n; x_c) f_j} = 1; \quad (15)$$

where the superscript $\pm = 1$ indicates the direction of the incident particle. In our calculation, a large enough cutoff to the sideband index is imposed. The $r_m^{(+)}(n; x_c); t_m^{(+)}(n; x_c)$ coefficients that we obtain are exact in the numerical sense.

The current transmission coefficient $T_{nm}(E; x_c)$ is the ratio between the transmitting current in the m th sideband and the corresponding incident current due to a n th subband electron, with incident energy E , and incident direction \pm . This current transmission coefficient is related to the transmission coefficient, given by

$$T_{nm}(E; x_c) = \frac{j_m^{(+)}(E_n; x_c) f_j \exp \frac{m}{4!x}}{\frac{\frac{1}{4} + i \frac{E_n+m}{4!x}}{\frac{1}{4} + i \frac{E_n}{4!x}}} \quad (16)$$

where $E_n = E - \frac{n}{4!x}$. The total current transmission coefficient $T^{\pm}(E; x_c)$ is defined as

$$T^{\pm}(E; x_c) = \sum_n T_n^{\pm}(E; x_c) = \sum_n \sum_m T_{nm}^{\pm}(E; x_c); \quad (17)$$

Furthermore, in the case when the saddle-point potential is shifted by U , the total current transmission coefficient becomes $T^{\pm}(E - U; x_c)$.

We find that the total current transmission coefficients $T^{+}(E; x_c)$ and $T^{-}(E; x_c)$ are different for $x_c \neq 0$, when the interaction region is not centered at the symmetric center of the constriction. This can be understood from the following example, when the entire interaction region is, say, on the right hand side of the constriction and the incident energy E is chosen such that the electrons have to tunnel through the constriction. In this example, an electron incident from the left hand side receives no assistance from the time-modulated gate-voltage when tunneling through the constriction. Rather, the electron suffers additional reflection from the gate-voltage after tunneling through the constriction. However, for an electron incident from the right hand side, it can receive assistance from the gate-voltage when passing through the

constriction. Of course, the electron might be reflected by this gate-voltage as well. But in the opening up of a new gate-voltage-assisted transmission channel, when the electron, after absorbing $m\hbar$, can propagate, rather than tunneling, through the constriction, the assisted feature dominates. This example, though not a generic one, illustrates that the difference between the current transmission coefficients originates from the different extent the time-modulated gate-voltage involves in assisting the transmitting electrons.

The fact that $T^{+}(E; x_c)$ can be different from $T^{-}(E; x_c)$, when the QPC is acted upon by a time-modulated potential, leads to a nonzero current in an unbiased QPC. The current is the photocurrent I_{ph} (see below). Therefore, the transport in the QPC is better represented by the differential conductance G , rather than the conductance, or the total current transmission coefficients T .

To find the differential conductance in the low-bias regime, we choose the left reservoir to be the source electrode such that the left reservoir has a chemical potential shift of $(1 - \frac{1}{2})\phi$, and the right reservoir has a chemical potential shift of $\frac{1}{2}\phi$. In the low-bias regime, we have $\phi \ll \phi_0$. The parameter ϕ_0 had been adopted by Martin-Moreno et al.[25] and Ouchterlony et al.[26] in their work on the nonlinear dc transport through a saddle-point constriction. The current I in the constriction is then given by [27]

$$I = \frac{2e}{h} \int_{-\frac{1}{2}\phi}^{\frac{1}{2}\phi} dE f(E - \frac{1}{2}\phi) T^{+}(E; x_c) - \int_{-\frac{1}{2}\phi}^{\frac{1}{2}\phi} dE f(E + \frac{1}{2}\phi) T^{-}(E; x_c); \quad (18)$$

where $f(E) = [1 + \exp(E/k_B T)]^{-1}$ is the Fermi function. Here e is the charge of an electron. Assuming that the lowest energy electrons from the reservoirs contribute negligibly to I , we can extend the lower energy limit of the above integral to $-\infty$. The zero temperature limit of Eq. (18) is given by

$$I = \frac{2e}{h} \int_{-\infty}^{\frac{1}{2}\phi} dE T^{+}(E; x_c) - \int_{-\infty}^{\frac{1}{2}\phi} dE T^{-}(E; x_c); \quad (19)$$

The differential conductance in the low bias regime, defined by

$$G_0 = \frac{\partial I}{\partial V_{sd}} \bigg|_{V_{sd}=0}; \quad (20)$$

can be calculated from differentiating Eq. (19), and is given by

$$G_0 = \frac{2e^2}{h} T^{+}(\frac{1}{2}\phi; x_c) (1 - f(\frac{1}{2}\phi; x_c)) + T^{-}(\frac{1}{2}\phi; x_c) f(\frac{1}{2}\phi; x_c); \quad (21)$$

It is interesting to note that G_0 depends on ϕ whenever $T^{+}(\frac{1}{2}\phi; x_c) \neq T^{-}(\frac{1}{2}\phi; x_c)$, and that this ϕ -dependence in

G_0 does not occur for the cases of purely elastic scatterings, such as impurity scatterings. We expect G_0 to be the major contribution to the differential conductance G . The other contribution to G is from the change in the photocurrent I_{ph} when the QPC is subjected to the low-biased transport field. This term is much smaller than G_0 and is qualitatively given by

$$G_{ph} = \frac{e}{2! \frac{2}{x} L} \frac{\partial}{\partial x_c} I_{ph}(\epsilon; x_c); \quad (22)$$

where

$$I_{ph}(\epsilon; x_c) = \frac{2e}{h} \sum_1^Z dE T^+(E; x_c) T^-(E; x_c) \quad (23)$$

is the photocurrent. Here L is the effective length of the potential drop across the QPC, and $\epsilon = (2! \frac{2}{x} L)$ is the effective shift of the QPC position caused by the small bias potential. The differential conductance $G = G_0 + G_{ph}$.

III. NUMERICAL EXAMPLES

In our numerical examples, the physical parameters are taken to be that in a high-mobility GaAs AlGaAs heterostructure, with a typical electron density $n = 2.5 \times 10^{11} \text{ cm}^{-2}$ and $m = 0.067 m_e$. Correspondingly, we choose an energy unit $E = \hbar^2 k_F^2 / (2m) = 9 \text{ meV}$, a length unit $a = 1/k_F = 79.6 \text{ \AA}$, and a frequency unit $\omega = E/\hbar = 13.6 \text{ THz}$. For the saddle-point constriction, we have chosen $\epsilon_x = 0.0125$, and $\epsilon_y = 0.05$ such that the effective length to width ratio of the constriction is $L_c/W_c = \epsilon_y/\epsilon_x = 4$. In presenting the dependence of G on ϵ , it is more convenient to plot G as a function of X , where

$$X = \frac{1}{2} \frac{\epsilon}{\epsilon_y} + 1; \quad (24)$$

The integral value of X is the number of propagating channels through the constriction.

To evaluate the term G_{ph} of the differential conductance G , the length L of the potential drop is taken to be of the same order as L_c [28], where the length of our constriction $L_c = 4W_c = 8 \times \frac{3}{4} \epsilon_y = 62$ for a typical $n = 1$ subband. Following Ouchterlony et al., who have chosen $L_c = L = 1.5$ [29], we choose L to have a value $L = L_c = 1.5 \times 41$.

In Figs. 2, 3, and 4, we present the changes in the G characteristics when the range of the time-modulated potential is increased, from $a = 16; 32$; to 50 , respectively. All these time-modulated potentials are centered, with $x_c = 0$, and have the same frequency ($\omega = 0.04$), and the same amplitude ($V_0 = 0.06$). The bias parameter $\epsilon = 0.5$ in these figures. The G characteristics are represented by the dependence of G on X , the suitably

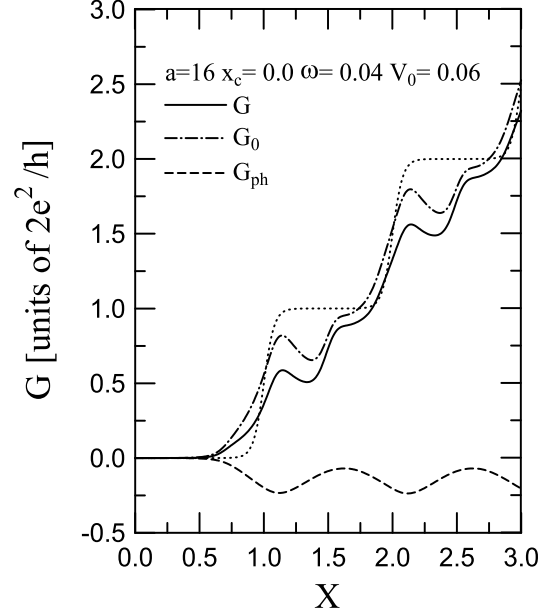


FIG. 2: Differential conductance G as a function of X for a centered time-modulated potential ($x_c = 0$), with oscillating amplitude $V_0 = 0.06$, frequency $\omega = 0.04$, and $\epsilon = 0.5$. The range of the potential $a = 16$ covers a distance up to $d = 8$ from the constriction center. The solid curve is the total differential conductance G , the dashed-dotted curve is G_0 , and the dashed curve is G_{ph} . In the assisted regime, G_{ph} suppresses the differential conductance, but the general tunneling-like feature remains unchanged. In the suppressed regime, there are dip structures at $X = 1.4$; and 2.4 .

rescaled chemical potential ϵ . According to this scale, when ϵ is changed by a subband energy spacing, it corresponds to $X = 1$, and when ϵ is changed by $\hbar\omega$, it corresponds to $X = \epsilon/\hbar\omega = (2! \epsilon_y) = 0.4$. In addition, when $X = N$, ϵ is at the threshold of the N th subband.

In Fig. 2, we find both gate-voltage-assisted and gate-voltage-suppressed features in G . These two features occur in well separated regions of X . The gate-voltage-assisted regions occur when ϵ is just beneath a subband threshold, and is most evident in the pinch-off ($X < 1$) region, while the gate-voltage-suppressed regions occur when ϵ is above but close to a subband threshold. Dip structures are found in the suppressed region, at around $X = 1.4$; and 2.4 , that is, at $X = 0.4$ above a threshold. These dip structures are due to the processes that an electron in the N th subband, at energy $N + X$, can give away an energy $\hbar\omega$ and become trapped in the quasi-bound-state (QBS) just beneath the threshold [17, 21]. In contrast with the QBS features in narrow channels [21], the QBS structures in a saddle-point constriction is much broader, indicating that the QBS lifetime is much shorter due to the added possibility of escape via tunneling. In the gate-voltage-assisted region, G increases gradually, rather than abruptly, when a channel, after picking up an energy $\hbar\omega$, becomes propagating.

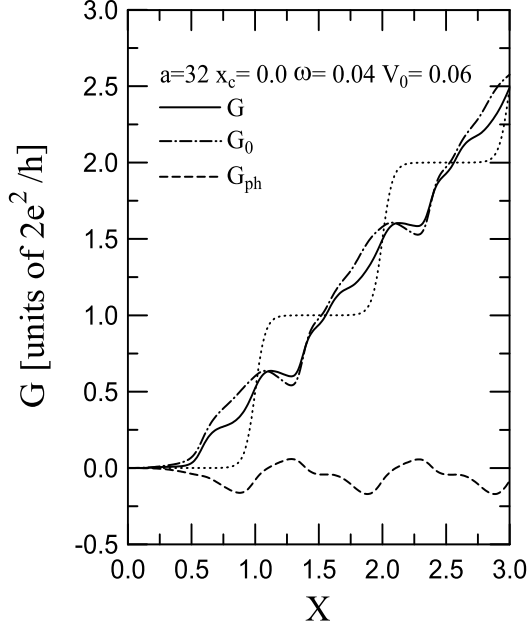


FIG. 3: Differential conductance G as a function of X for a centered time-modulated potential. The physical parameters are the same as in Fig. 2 except that the range of the potential is $a = 32$. The potential covers a distance up to $d = 16$ from the constriction center. In the assisted regime, the G_{ph} modifies the shoulder-like feature in G_0 and leads to the quasi-ministep-like feature in G . In the suppressed regime, the dip structures at $X = 1.4$; and 2.4 are slightly modified by G_{ph} .

This is because the range of the interacting region does not cover far enough so that the electron, though having the right energy, has to tunnel to the interacting region first before being assisted. This also explains why there are no structures at $N = 2X$, which corresponds to the $2h\hbar$ processes. Consequently, the dip structures in the suppressed regions are not affected by the gate-voltage-assisted features.

It is interesting to note that there is no harmonic feature that could have been caused by the abrupt profile of the gate-voltage. This is because the effective wavelength of a particle decreases as it emanates from the constriction so that multiple scattering between the two abrupt edges of the potential is subjected to rapid phase fluctuations, suppressing any possible harmonic resonances. Thus our results should represent also the cases of smooth-profile gate-voltages.

In Fig. 3, the QBS structures at $X = 1.4$; and 2.4 are still evident. The assisted features are enhanced. In particular, in the pinch-off region, G increases much faster, showing a ministep-like structure. The gate-voltage-assisted and the gate-voltage-suppressed features are well separated because no $2h\hbar$ features are found.

In Fig. 4, there are additional dip structures in G_0 at $X = 1.8$; and 2.8 , which indicates that $2h\hbar$ processes become significant. There are, of course, assisted features that involve one $h\hbar$ processes, and they are the

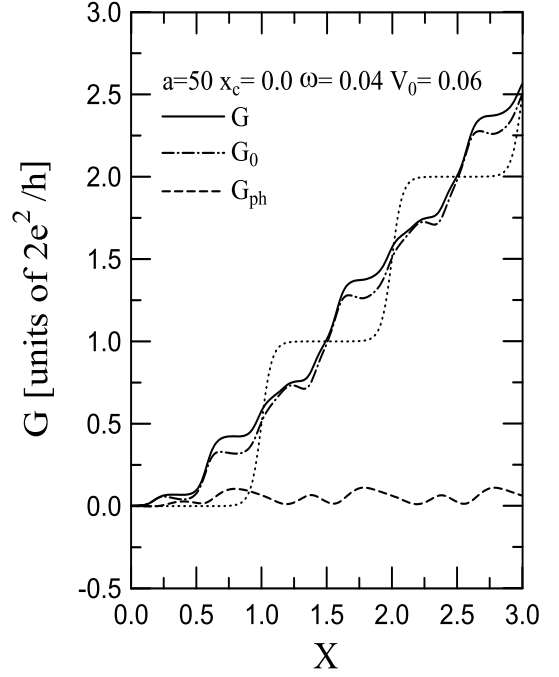


FIG. 4: Differential conductance G as a function of X for a centered time-modulated potential. The physical parameters are the same as in Fig. 2 except that the range of the potential is $a = 50$, which covers a distance up to $d = 25$ from the constriction center. In the assisted regime, G_{ph} enhances G . There are two ministep-like structures in the pinch-off region.

abrupt rises in G at $X = 0.6$; 1.6 ; and 2.6 . The assisted feature that involves $2h\hbar$ is most clearly demonstrated in the pinch-off region, around $X = 0.2$, where G exhibits another ministep. Other $2\hbar$ assisted processes are at $X = 1.2$; and 2.2 , which, unfortunately, are in the vicinity of the dip structures at $X = 1.4$; and 2.4 . Hence the dip structures become less dip-like but have turned into a sharp uplift in G , because they are affected by the assisted features.

The assisted features in the above three figures are different, and the difference is associated with how the electrons enter the interaction region. For the N th subband electrons with incident energies that fall within the $m\hbar$ interval below the threshold of the same subband, they are nonpropagating. They can become propagating, and traverse through the constriction, by absorbing $m\hbar$ from the time-modulated potential. But the electrons have to be in the interaction region to absorb the needed energy. If the gate-voltage covers a region over a distance $d > d_m = \frac{p}{m\hbar} = \frac{1}{x}$ from the center, and on the incident side, of the constriction, the incident electrons can propagate into the interaction region. However, if the gate-voltage only covers regions over a shorter distance ($d < d_m$) from the constriction center, the electrons have to tunnel into the interaction region. For $x = 0.0125$, we have $d_1 = 16$, and $d_2 = 23$. We recall that the distances d covered by the gate-voltage are $d = 8$; 16 ; and 25 , respec-

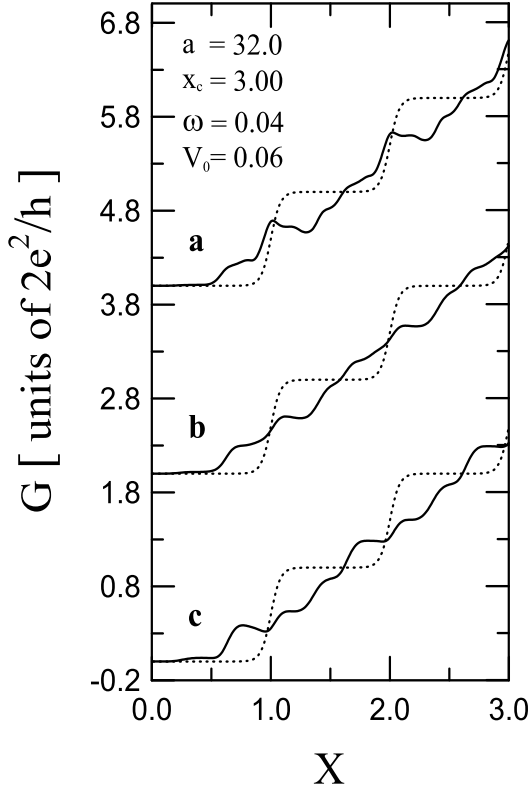


FIG. 5: Differential conductance G as a function of X for an o-centered time-modulated potential ($x_c = 3$), with range $a = 32$, frequency $\omega = 0.04$, and oscillating amplitude $V_0 = 0.06$. The parameter $\gamma = 0.2$ (a); 0.5 (b); and 0.8 (c). The curves are vertically offset for clarity.

tively, in Figs. 3, 4, and 5. Hence in Fig. 2, $d < d_1$, and the electrons have to tunnel into the interaction region so that the assisted feature, such as in the $X \approx 1$ region, exhibits a tunneling-like structure. In Fig. 3, when $d = d_1$, the electrons can barely avoid entering the interaction region via tunneling, the assisted feature exhibits a quasi-mini-step-like structure. In Fig. 4, when $d > d_2$, the electrons involving in the $2h!$ processes can also propagate into the interaction region, and the assisted feature exhibits additional mini-step structures.

In Fig. 5, we present the dependence of the G characteristics on the parameter γ . The time-modulated gate-voltage is o-centered, with $x_c = 3.0$, range $a = 32$, $V_0 = 0.06$, and frequency $\omega = 0.04$. The parameter $\gamma = 0.2$; 0.5 ; and 0.8 in Figs. 5(a), (b), and (c), respectively. The curves in Fig. 5 show that G is quite sensitive to γ . But from further analysis, we find that it is G_0 , rather than G_{ph} , that gives rise to the γ -sensitivity in G . Hence, according to Eq. (18), as γ increases, the contribution to G_0 from T^+ decreases while that from T^- increases. Since the assisted feature of T^- is prominent than that of T^+ because $x_c = 3.0$, therefore the assisted features in the pinch-off region are enhanced progressively in Figs. 5(a), (b), and (c). This particular γ -

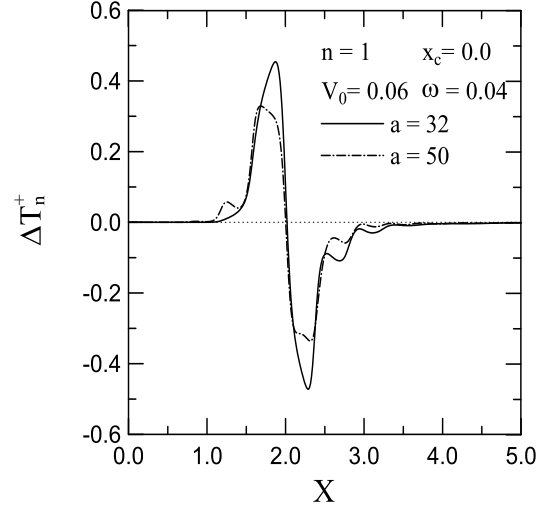


FIG. 6: T_n^+ as a function of X for a centered time-modulated potential and subband $n = 1$, with frequency $\omega = 0.04$, $\gamma = 0.5$, and oscillating amplitude $V_0 = 0.06$. The potential range $a = 32$ (solid); and 50 (dashed-dotted). The assisted feature is found below $X = 2$ (the $n = 1$ subband edge), and the suppressed feature is found above $X = 2$. The $2h!$ structures appear in the longer potential range ($a = 50$) case. The QBS features are at around $X = 2.4$; 2.8 ; and 3.2 .

dependence simply reflects the asymmetry in $T^+(\gamma; x_c)$ and $T^-(\gamma; x_c)$, which occurs for coherent inelastic scatterings and not for elastic scatterings.

IV. CONCLUSION

We have shown that the differential conductance G , rather than the conductance or the current transmission coefficient, is the relevant physical quantity for the characterization of the low-bias transport, when the QPC is acted upon by a time-modulated field. This has not been recognised previously. Thus to compare with the results of previous studies, we can only turn to the current transmission coefficient. The deviation of the current transmission coefficient from its unperturbed value

$$T_n^+(\epsilon; x_c) = T_n^+(\epsilon; x_c) - T_n^0(\epsilon);$$

was the photoconductance calculated by Grinwaig et al.[8], and Maa et al.[10], when they considered a transverse electric field acting on a QPC with varying width. Here $T_n^0(\epsilon) = 1/[1 + \exp(-\epsilon/\epsilon_n)]$, and n is the subband index of the incident electron. In Fig. 6, we plot our $T_n^+(\epsilon; x_c)$ results against X . The time-modulated potential is centered ($x_c = 0$), the frequency $\omega = 0.04$, the amplitude $V_0 = 0.06$, and the incident subband index $n = 1$. The threshold for the subband is $X = 2$. The assisted and the suppressed features are clearly shown below and above the threshold, respectively. This trend is the same as the results of Refs. 8, and 10, even though

the inelastic processes induced by a transverse field is different from that by a potential. On the other hand, our results have the added QBS features in the suppressed region, and the added $2!$ feature in the assisted region for a longer potential range. Both features are the main results of this paper.

Finally, we have demonstrated the robustness of the QBS features. Should these QBS features exist and remain robust in the cases of time-modulated electric field?

We are currently investigating this possibility.

Acknowledgments

This work was supported in part by the National Science Council of the Republic of China through Contract No. NSC 86-2112-M-009-004.

-
- [1] F. Hekking, and Y. V. Nazarov, Phys. Rev. B 44 (1991) 11506.
- [2] Q. Hu, Appl. Phys. Lett. 62 (1993) 837.
- [3] S. Feng, and Q. Hu, Phys. Rev. B 48 (1993) 5354.
- [4] R. A. Wyss, C. C. Eugster, J. A. del Alamo, and Q. Hu, Appl. Phys. Lett. 63 (1993) 1522.
- [5] L. Fedichkin, V. Ryzhii, and V. V. Yurkov, J. Phys. Condens. Matter 5 (1993) 6091.
- [6] T. J. B. M. Janssen, J. C. M. M. Janssen, J. Singleton, N. K. Patel, M. Pepper, J. E. F. Frost, D. A. Ritchie, and G. A. C. Jones, J. Phys. Condens. Matter 6 (1994) L163.
- [7] L. Y. Gorelik, A. Grincwaj, V. Z. Kliner, R. I. Shekhter, and M. Jonson, Phys. Rev. Lett. 73 (1994) 2260.
- [8] A. Grincwaj, L. Y. Gorelik, V. Z. Kliner, and R. I. Shekhter, Phys. Rev. B 52, 12168 (1995).
- [9] C. S. Chu, and C. S. Tang, Solid State Commun. 97 (1996) 119.
- [10] F. A. M. M. , and L. Y. Gorelik, Phys. Rev. B 53 (1996) 15885.
- [11] V. A. Chitta, C. Kutter, R. E. M. de Bekker, J. C. M. M. Janssen, S. J. Haworth, J. M. Chamberlain, M. Henin, and G. Hill, J. Phys. Condens. Matter 6 (1994) 3945.
- [12] M. Wagner, Phys. Rev. Lett. 76 (1996) 4010.
- [13] M. Buttiker, and R. Landauer, Phys. Rev. Lett. 49 (1982) 1739.
- [14] D. D. Coon, and H. C. Liu, J. Appl. Phys. 58 (1985) 2230.
- [15] X. P. Jiang, J. Phys. Condens. Matter 2 (1990) 6553.
- [16] M. Y. Azbel, Phys. Rev. B 43 (1991) 6847.
- [17] P. F. Bagwell, and R. K. Lake, Phys. Rev. B 46 (1992) 15329.
- [18] F. Rojas, and E. Cota, J. Phys. Condens. Matter 5 (1993) 5159.
- [19] M. Wagner, Phys. Rev. B 49 (1994) 16544; Phys. Rev. A 51 (1995) 798.
- [20] O. A. Tkachenko, V. A. Tkachenko, and D. G. Baksheyev, Phys. Rev. B 53 (1996) 4672.
- [21] C. S. Tang, and C. S. Chu, Phys. Rev. B 53 (1996) 4838.
- [22] L. Y. Gorelik, A. Grincwaj, V. Z. Kliner, R. I. Shekhter, and M. Jonson, Phys. Rev. Lett. 73 (1994) 2260.
- [23] C. S. Chu, and M. H. Chou, Phys. Rev. B 50 (1994) 14212.
- [24] M. Abramowitz and I. A. Stegun, Handbook of Mathematical Functions, Dover, New York, 1972, p. 504.
- [25] L. Martin-Moreno, J. T. Nicholls, N. K. Patel, and M. Pepper, J. Phys. Condens. Matter 4 (1992) 1323.
- [26] T. Ouchterlony, and K. F. Berggren, Phys. Rev. B 52 (1995) 16329.
- [27] One may want to use another current expression, which, in units of $2e\hbar$, is given by
- $$I = \sum_{n=1}^{\infty} \frac{dE}{dE_{nm}} T_{nm}^+ (E; x_c) f(E_{nm}) \left[1 - f(E_{nm} + \dots) \right] \\ T_{nm} (E; x_c) f(E_{nm} + \dots) \left[1 - f(E_{nm} - \dots) \right] g :$$
- However, it can be shown that the two expressions give the same result.
- [28] I. B. Levinson, Zh. Eksp. Teor. Fiz. 95 (1989) 2175 [Sov. Phys. JETP 68 (1989) 1257].
- [29] In Ref. 26, Ouchterlony et al. have chosen the parameters: $m = 0.2m_e$, $\hbar^2 V_y = 9 \text{ meV}$, and $\hbar^2 x = 4.5 \text{ meV}$. Their length $L_c = 4\hbar^2 V_y / (m \hbar^2 V_y) = 11.3 \text{ nm}$ for a typical $n = 1$ subband. The length L over which the potential drop occurs was taken to be $L = 30 \text{ nm}$. Thus, in Ref. 26, $L_c = L/1.5$.